Mon. Not. R. Astron. Soc. **399,** L156–L159 (2009) doi:10.1111/j.1745-3933.2009.00743.x

On Type Ia supernovae from the collisions of two white dwarfs

Cody Raskin,[1⋆] F. X. Timmes,[1,2] Evan Scannapieco,[1] Steven Diehl[3] and Chris Fryer[3]

[1] *School of Earth and Space Exploration, Arizona State University, Tempe, AZ 85287-1404, USA*
[2] *Joint Institute for Nuclear Astrophysics, Notre Dame, IN 46556-5670, USA*
[3] *Los Alamos National Laboratories, Los Alamos, NM 87545, USA*

Accepted 2009 August 14. Received 2009 August 12; in original form 2009 July 21

ABSTRACT

We explore collisions between two white dwarfs as a pathway for making Type Ia supernovae (SNIa). White dwarf number densities in globular clusters allow 10–100, redshift $\lesssim$1 collisions per year, and observations by Chomiuk et al. of globular clusters in the nearby S0 galaxy NGC 7457 have detected what is likely to be a SNIa remnant. We carry out simulations of the collision between two 0.6 $M_\odot$ white dwarfs at various impact parameters and mass resolutions. For impact parameters less than half the radius of the white dwarf, we find such collisions produce $\approx$0.4 $M_\odot$ of ^{56}Ni, making such events potential candidates for underluminous SNIa or a new class of transients between Novae and SNIa.

Key words: hydrodynamics – nuclear reactions, nucleosynthesis, abundances – supernovae: general – white dwarfs.

1 INTRODUCTION

Type Ia supernovae (SNIa) play a key role in astrophysics as premier distance indicators for cosmology (Phillips 1993; Riess et al. 1998; Perlmutter et al. 1999), as direct probes of low-mass star formation rates at cosmological distances (Scannapieco & Bildsten 2005; Mannucci, Della Valle & Panagia 2006; Maoz 2008) and as significant contributors to iron-group elements in the cosmos (Wheeler, Sneden & Truran 1989; Timmes, Woosley & Weaver 1995; Feltzing, Holmberg & Hurley 2001; Strigari 2006). Our current understanding is that there are two major progenitor systems for these events. The first possibility, the single-degenerate scenario, consists of a carbon–oxygen white dwarf in a binary system evolving to the stage of central ignition by mass overflow from a low-mass stellar companion (Whelan & Iben 1973; Nomoto 1982; Hillebrandt & Niemeyer 2000). The second possibility, the double-degenerate scenario, consists of the merger of two white dwarfs in a binary system (Iben & Tutukov 1984; Webbink 1984; Yoon, Podsiadlowski & Rosswog 2007). It is unknown at what relative frequency both of these channels operate (Livio 2000; Maoz 2008).

Collisions between two white dwarfs are likely to happen less frequently than binary mergers. However, as discussed in Timmes (2009) and Rosswog et al. (2009), they will occur in globular clusters where the stellar densities are extremely high. For a typical globular cluster velocity dispersion of $\approx$5–10 km s^{-1}, and a white dwarf escape velocity of $\approx$4000 km s^{-1}, the physical cross-section of equal-mass white dwarfs is enhanced by a factor of 4×10^4–2×10^5 by gravitational focusing. For an average globular cluster mass of 10^6 $M_\odot$ (Brodie & Strader 2006), a Salpeter initial mass function (Salpeter 1955) and a globular cluster core radius of 1.5 pc (Peterson & King 1975), we conservatively estimate an average white dwarf number density in globulars to be $\approx 10^4$ pc^{-3}, and estimating that about 1/1000 of the average 5×10^8 $M_\odot$ per Mpc^{-3} stellar mass density in the Universe is in globular clusters (see Pfahl, Scannapieco & Bildsten 2009 and references therein) the overall rate of such collisions is about 5–20 $\times$ 10^{-10} per comoving Mpc^3 per year. This corresponds to 10–100, $z \lesssim 1$ collisions per year. Note that this calculation depends in detail on the minimum impact parameter that leads to explosive nuclear burning, as studied in detail below. Our estimate is significantly lower than a recently submitted paper (Rosswog et al. 2009), primarily due to the assumed core radius of globular clusters.

Beyond $\approx$50 Mpc, current surveys are not sufficiently accurate to distinguish between supernovae in globular clusters from those that arise from galaxy field stars in front of or behind globular clusters (Pfahl et al. 2009). Furthermore, observations of globular clusters in the nearby S0 galaxy NGC 7457 have detected what is likely to be a remnant of a SNIa (Chomiuk et al. 2008). Taken together, these estimates and observations suggest that white dwarf collisions are likely to appear in current and future SNIa samples. As double-degenerate supernovae from collisions may not fit the standard templates, SN surveys may have to consider possible contamination from double-degenerate collisions that masquerade as traditional SNIa.

In this Letter, we begin to examine collisions between two white dwarfs as a pathway for producing SNIa. In Section 2, we describe our simulations of the impact between two 0.6 $M_\odot$ white dwarfs, and in Section 3 we discuss the resulting hydrodynamics, thermodynamics and nucleosynthesis. In Section 4, we speculate on other mass pairs and impact parameters and discuss the implication of our results.

⋆E-mail: cody.raskin@asu.edu

Table 1. Simulation impact parameters, b, d and total particle count, N.

Scenario	b [$R_\odot$]	$d(R_{wd})$	N (x1000)
1	0	0	800
2	0.9	0.5	800
3	1.7	0.9	200

2 SNSPH SIMULATIONS

All of our simulations are conducted with a three-dimensional (3D) smooth particle hydrodynamics code, SNSPH (Fryer, Rockefeller & Warren 2006). In collision scenarios with a non-zero impact parameter, angular momentum plays a critical role in the final outcome, and Lagrangian particle methods generally conserve angular momentum better than Eulerian grid methods. We added a 13-isotope α-chain nuclear reaction network (Timmes 1999; Fryxell et al. 2000; Timmes, Hoffman & Woosley 2000a) and a Helmholtz free energy based stellar equation of state (Timmes & Arnett 1999; Timmes & Swesty 2000) to SNSPH to construct the initial white dwarf models and run our collision models.

Our initial 0.6 $M_\odot$ white dwarf is composed of equal parts ^{12}C and ^{16}O and is created using the Weighted Voronoi Tessellations method (Diehl & Statler 2006), which arranges particles in the configuration corresponding to the lowest energy state that is consistent with a given equation of state. The resulting white dwarfs have only minor temperature variations around 1×10^7 K. Any evolution the white dwarfs experience before the collision, then, is due only to their mutual gravitational interaction. We use a simple two-body solver to calculate the relative velocities of the two white dwarfs immediately before a collision for a given impact parameter and an initial relative velocity of 10 km s^{-1}, which corresponds to the typical virial velocity of a globular cluster. The velocities calculated by our two-body solver then serve as the initial conditions for our collision simulations.

Various angles of incidence for the collision were chosen. In Table 1, the initial impact parameter, b, is the vertical separation of the centres of the white dwarfs in terms of $R_\odot$ at a horizontal separation of ∞. Due to gravitational focusing, the final impact parameter, d, the vertical separation at the moment of collision, is significantly smaller and is given in Table 1 in terms of the radius of a 0.6 $M_\odot$ white dwarf, $\approx$0.01 $R_\odot$. The number of particles N in each model is also given in Table 1, i.e. there are $N/2$ particles per white dwarf.

3 RESULTS

3.1 Scenario 1

Snapshots of planar slices from the head-on collision case are given in Fig. 1. This extremely unlikely, but physically instructive, scenario was presented in Timmes (2009) and has also recently been explored in Rosswog et al. (2009). As the white dwarfs approach each other, their velocities increase to the escape speed, $\approx$4000 km s^{-1} (first panel). When the two white dwarfs first make contact (second panel), shock waves develop that attempt to travel outwards along the x-axis at roughly the sound speed, $\approx$3000 km s^{-1} (also see Fig. 2). The near equality of these two characteristic speeds means the shock waves stall as material falls through them (Fig. 1, third panel). The region between the two fronts achieves a nearly constant temperature ($T \sim 10^9$ K) and density

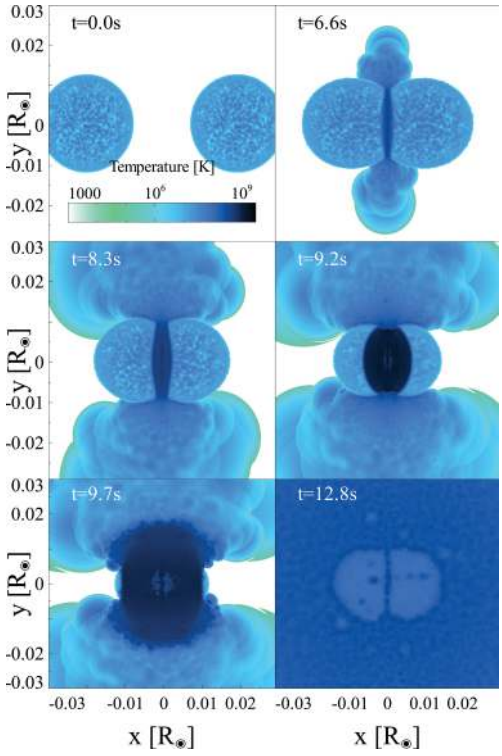

Figure 1. Planar slices through the 3D calculation of the evolution of head-on white dwarf collision Scenario 1, given in Table 1. The features of each panel are described in detail in Section 3.1. The sequence displayed, after the white dwarfs have collided in panel 2, takes place over a period of $\approx$6 s.

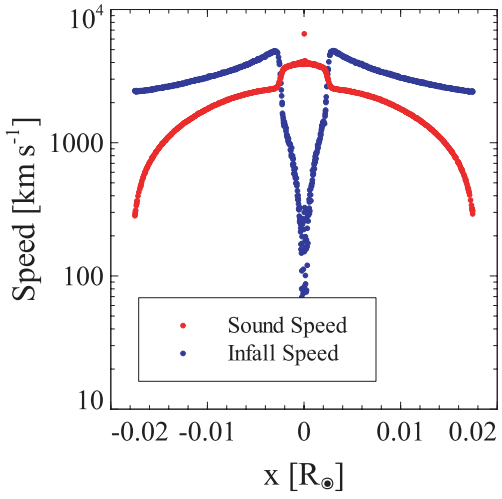

Figure 2. The sound speed and infall speed of particles lying on the x-axis in Scenario 1. This snapshot corresponds to panel 3 in Fig. 1. The material falling into the shocked region is moving at or above the sound speed for this region, causing the shock to stall.

($\rho \sim 10^6$ g cm^{-3}) with a non-explosive, mild rate of nuclear burning. This shocked region expands very slowly as more material piles into it. In this regime, the nuclear energy-generation rate scales as $\dot{\epsilon} \approx \rho^2\, T^{27}$.

When the high-density ($\approx 4 \times 10^6$ g cm^{-3}) central core of each white dwarf encounters the leading edge of the shock, it raises the energy-generation rate of enough material above the threshold needed to trigger a detonation (see Gamezo et al. 1999 and

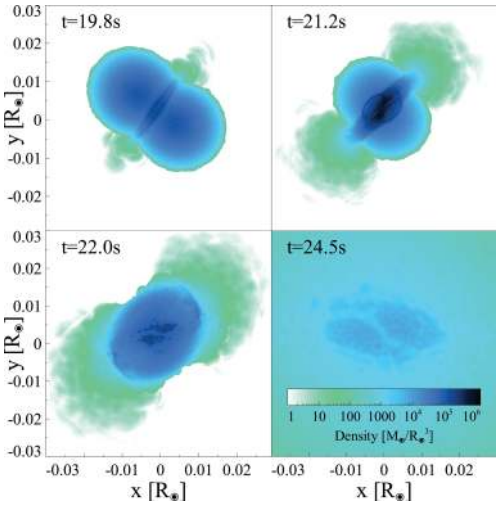

Figure 3. Planar slices through the 3D calculation of the evolution of the $d = 0.5\,R_{\rm wd}$ white dwarf collision Scenario 2, given in Table 1. The features of each panel are described in detail in Section 3.2.

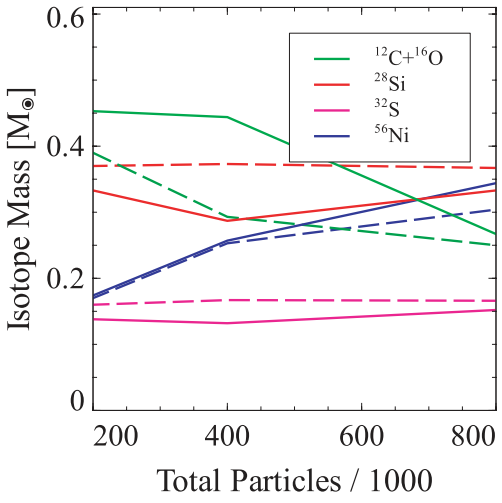

Figure 4. Isotope yields versus total particle count for Scenarios 1 and 2. The solid lines are the isotope yields of the head-on simulation, while the dashed lines are those of the $d = 0.5\,R_{\rm wd}$ simulation.

references therein). Two curved detonation fronts with $T \sim 10^{10}$ K form at the interfaces of the shocked and unshocked regions and begin to propagate (fourth panel in Fig. 1) which releases enough energy to unbind the merged system (fifth panel). The entire system then undergoes homologous expansion (sixth panel), leaving a small amount of unburned CO in the central regions surrounded by a layer of ^{56}Ni and other iron-group elements, a layer of Si-group elements and then an outer region of unburned CO. The final tally, with 1.2 $M_\odot$ of CO entering the system, is 0.34 $M_\odot$ of ^{56}Ni, 0.33 $M_\odot$ of ^{28}Si and 0.15 $M_\odot$ of unburned CO with the remaining mass distributed among other heavy elements (also see Fig. 4). Such an event, whose total mass is sub-Chandrasekhar, would be a potential candidate for either an underluminous SNIa or a new class of transients between Novae and SNIa.

3.2 Scenario 2

In Scenario 2, we use an impact parameter of $b = 0.9\,R_\odot$ in order to bring the stars into contact with a final impact parameter of $d = 0.5\,R_{\rm wd}$ or $d \approx 0.005\,R_\odot$. As in Scenario 1, the shock front stalls as the inward falling material is travelling at a comparable speed (first panel of Fig. 3). Once again, when the cores of the white dwarfs enter the shocked region, two detonation fronts break out and unbind the system (second panel). However, in this case, the additional torque applied to the shocked region as the stars continue to move past each other results in off-axis and off-centre detonation fronts that occur at earlier times than in Scenario 1 (second and third panels). In this case, 0.30 $M_\odot$ of ^{56}Ni and 0.37 $M_\odot$ of ^{28}Si are created, leaving 0.25 $M_\odot$ of unburned CO with the remaining mass distributed among other heavy elements.

3.3 Scenario 3

In Scenario 3, we increase the impact parameter to $b = 1.7\,R_\odot$, resulting in a pre-collision impact parameter of $d = 0.9\,R_{\rm wd}$ or $d \approx 0.009\,R_\odot$. This ensures a purely grazing incident, which is likely to be the most frequent impact scenario as a wide range of impact parameters will result in a similar, grazing collision when tidal effects transfer angular momentum from passing impactors. Absent the violent shock experienced in Scenarios 1 and 2, there is negligible nuclear burning in a purely edge-on impact. Less than 10^{-3} $M_\odot$ of ^{56}Ni are produced by the initial interaction. The kinematics of the collision causes both stars to become unbound, forming a rotating disc of white dwarf debris, which will eventually collapse into a single compact object as it cools.

3.4 Convergence studies

A known weakness of smooth particle hydrodynamic simulations is resolving shocks with a finite number of particles. For this reason, we carried out a convergence study of the $d = 0$ (Scenario 1) and $d = 0.5\,R_{\rm wd}$ (Scenario 2) cases in order to place upper limits on the isotope yields. Fig. 4 shows that with increasing particle count, more of the CO is converted into ^{56}Ni and ^{28}Si, while the abundance of ^{32}S remains relatively constant. While we did not achieve an absolute convergence in our simulations, we can reasonably extrapolate an upper limit of 0.4 $M_\odot$ of ^{56}Ni for the head-on merger scenario and 0.35 $M_\odot$ in the $d = 0.5\,R_{\rm wd}$ scenario, where 1.2 $M_\odot$ of CO enters the system. In low-impact-parameter collision scenarios involving larger masses for the constituent white dwarfs, it is very likely that this yield would increase.

Rosswog et al. (2009) find 0.32 $M_\odot$ of ^{56}Ni for the head-on collision of two 0.6 $M_\odot$ white dwarfs with a smoothed particle hydrodynamics resolution of 2×10^5 particles. This is consistent with our highest resolution SNSPH model with 8×10^5 particles, but is inconsistent with our lower resolution SNSPH models. Rosswog et al. (2009) do not present a convergence study of their SNSPH models, and find significantly less ^{56}Ni is synthesized when they use the finite difference code FLASH (Fryxell et al. 2000). We are currently using FLASH to calculate the nucleosynthesis for the three impact parameter cases studied in this Letter to investigate this apparent discrepancy and to validate (or falsify) the ^{56}Ni yields from our SNSPH models (Hawley W. & Timmes F. X., in preparation).

4 DISCUSSION

Direct collisions between white dwarfs offer an unexplored mechanism for SNIa production within the double-degenerate family of progenitor models. Our simulations suggest that at low-impact parameters, the collision between the most common white dwarf

masses ($0.6\,M_\odot$) can result in explosive nuclear burning, even though the total mass involved is below the Chandrasekhar limit, and producing enough ^{56}Ni to result in a dim SNIa or be an example of a new class of transients between Novae and SNIa. It is likely that collisions between more massive white dwarfs with impact parameters less than a white dwarf radius will result in brighter events. Although our simulations are unable to resolve the exact physics that trigger detonations in an open environment, these details might not be critical for the overall nucleosynthesis in collision scenarios.

Rosswog et al. (2009) have reported that a low-resolution $b = 0$ collision of two $0.9\,M_\odot$ white dwarfs can produce enough ^{56}Ni to resemble the nuclear yields of a typical SNIa. As we have shown above for two $0.6\,M_\odot$ white dwarfs, the nuclear yields are sensitive to the impact parameter. Grazing incident collisions between more massive white dwarfs are likely to lead to similar configurations. The ultimate fate of these systems will, like their binary merger cousins, depend on the total mass, thermal and neutrino cooling rates, angular momentum transport rate, mass accretion rate on to the hot central object and any residual nuclear burning (Yoon et al. 2007). Further studies are needed to say which white dwarf collisions lead to double-degenerate SNIa or perhaps a new class of transients between Novae and SNIa.

ACKNOWLEDGMENTS

This work was supported by the National Science Foundation under grant AST 08-06720. All simulations were conducted using the Ira A. Fulton High Performance Computing Center, Arizona State University. We thank our referees for their suggestions and comments.

REFERENCES

Brodie J., Strader J., 2006, ARA&A, 44, 193
Chomiuk L., Strader J., Brodie J. P., 2008, AJ, 136, 234
Diehl S., Statler T. S., 2006, MNRAS, 368, 497
Feltzing S., Holmberg J., Hurley J. R., 2001, A&A, 377, 911
Fryer C. L., Rockefeller G., Warren M. S., 2006, ApJ, 643, 292
Fryxell B. et al., 2000, ApJS, 131, 273
Gamezo V. N., Wheeler J. C., Khokhlov A. M., Oran E. S., 1999, ApJ, 512, 827
Hillebrandt W., Niemeyer J. C., 2000, ARA&A, 38, 191
Iben J. I., Tutukov A. V., 1984, ApJS, 54, 335
Livio M., 2000, in Niemeyer J. C., Truran J. W., eds, Type Ia Supernovae, Theory and Cosmology. Cambridge Univ. Press, Cambridge
Mannucci F., Della Valle M., Panagia N., 2006, MNRAS, 370, 773
Maoz D., 2008, MNRAS, 384, 267
Nomoto K., 1982, ApJ, 253, 798
Perlmutter S. et al., 1999, ApJ, 517, 565
Peterson C., King J., 1975 AJ, 80, 427
Pfahl E., Scannapieco E., Bildsten L., 2009, ApJ, 695, L111
Phillips M. M., 1993, ApJ, 413, L105
Riess A. G. et al., 1998, AJ, 116, 1009
Rosswog S., Kasen D., Guillochon J., Ramirez-Ruiz E., 2009 ApJ, submitted (arXiv:0907.3196)
Salpeter E., 1955, ApJ, 121, 161
Scannapieco E., Bildsten L., 2005, ApJ, 629, L85
Strigari L. E., 2006, New Astron. Rev., 50, 566
Timmes F. X., 1999, ApJS, 124, 241
Timmes F. X., 2009, in Aubourg E., ed., SNIa Progenitors Workshop 2009, online proceedings (http://sn.aubourg.net/workshop09/pdf/timmes.pdf)
Timmes F. X., Arnett D., 1999, ApJS, 125, 277
Timmes F. X., Swesty F. D., 2000, ApJS, 126, 501
Timmes F. X., Woosley S. E., Weaver T. A., 1995, ApJS, 98, 617
Timmes F. X., Hoffman R. D., Woosley S. E., 2000, ApJS, 129, 377
Webbink R. F., 1984, ApJ, 277, 355
Wheeler J. C., Sneden C., Truran J. W., Jr, 1989, ARA&A, 27, 279
Whelan J., Iben I. J., 1973, ApJ, 186, 1007
Yoon S.-C., Podsiadlowski P., Rosswog S., 2007, MNRAS, 380, 933

This paper has been typeset from a TEX/LATEX file prepared by the author.